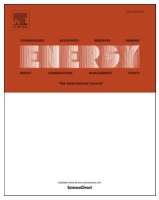
Energy 314 (2025) 134147



Contents lists available at ScienceDirect

Energy

journal homepage: www.elsevier.com/locate/energy



Thermodynamic analysis of decarbonizing NGCC power plants by the tail-end green ammonia-driven calcium looping

Song He [a,b,d], Xuelan Zeng [a,b,**,1], Yawen Zheng [b,c], Mingming Zhu [d,*,1], Dan Wang [e], Junyao Wang [f,g]

[a] Guangdong Basic Research Center of Excellence for Ecological Security and Green Development, Guangdong University of Technology, No.100 Waihuan Xi Road, Guangzhou, 510006, China
[b] Collaborative Innovation Institute of Carbon Neutrality and Green Development, Guangdong University of Technology, No.100 Waihuan Xi Road, Guangzhou, 510006, China
[c] China Shenzhen Gas Corporation Ltd. Shenzhen, 518040, China
[d] School of Water, Energy and Environment, Cranfield University, Cranfield, Bedfordshire, MK43 0AL, UK
[e] State Power Investment Group Hydrogen Energy Technology Development Co., Ltd, China
[f] School of Material and Energy, Guangdong University of Technology, Guangzhou, 510006, China
[g] Guangdong Provincial Key Laboratory of Functional Soft Matter, Guangzhou, 510006, China

ARTICLE INFO

Handling editor: Ruzhu Wang

Keywords:
Calcium looping
Ammonia
Thermochemical recuperation
Post-combustion CO_2 capture

ABSTRACT

This work proposes a novel ammonia driven tail-end calcium looping (CaL) process to capture carbon emission from natural gas combined cycle (NGCC) power plants for net-zero energy. Two integration schemes are introduced, including sensible heat thermochemical recuperation (SHTR) and carbonation heat thermochemical recuperation (CHTR) driven by combustion of partially cracked ammonia as a zero-carbon fuel. Results show that energy penalties can be reduced from 9.6 % in the NGCC power plant with the CaL-Oxy method to 1.8 % in the SHTR scheme and 1.4 % in the CHTR scheme, respectively. Comparing with the NGCC base power plant and the NH_3-based thermochemical recuperation power plant, energy savings can be achieved at 5.44 MJ_{LHV}/kg CO_2 in the SHTR scheme and 6.73 MJ_{LHV}/kg CO_2 in the CHTR scheme. Additionally, exergy analysis shows that the reduction of exergy destruction in the carbonation and calcination processes determines the thermodynamic performance enhancement. Cascaded heat recovery of carbonation heat and the heating supply method of calcination narrow the energy level difference, contributing to the reduction of exergy destruction. Sensitivity analysis indicates that reorganizing a more efficient thermodynamic cycle can offset the energy consumption of CO_2 capture from flue gas, resulting in an optimized negative energy penalty at −0.8 %.

Nomenclature

A	Energy level
A_{ed}	Energy level of donors
A_{ea}	Energy level of acceptors
ASU	Air separation unit
CaL	Calcium looping
CaL-Oxy	Calcium looping with oxy-fuel combustion
CCR	CO_2 capture ratio
CCUS	CO_2 capture, utilization and storage
CE	CO_2 emission intensity of power plants
CHTR	Carbonation heat thermochemical recuperation
E_{Re}	Renewable electricity input
EUD	Energy utilization diagram
Δ E	Exergy change
EX_{ch}	Chemical exergy
EX_{des}	Exergy destruction
EX_{in}	Exergy input
EX_{out}	Exergy output
FWH	Feedwater heater
GT	Gas turbine
Δ H	Enthalpy change
HRSG	Heat recovery steam generator

(*continued on next column*)

(*continued*)

(*continued on next page*)

** Corresponding author. Guangdong University of Technology, No.100 Waihuan Xi Road, Guangzhou, 510006, China.
* Corresponding author. Cranfield University, Cranfield, Bedfordshire, MK43 0AL, UK.
E-mail addresses: zengxuelan@gdut.edu.cn (X. Zeng), mingming.zhu.152@cranfield.ac.uk (M. Zhu).
[1] These authors have the same contribution to this study.

https://doi.org/10.1016/j.energy.2024.134147
Received 5 August 2024; Received in revised form 9 October 2024; Accepted 7 December 2024
Available online 8 December 2024
0360-5442/© 2024 The Authors. Published by Elsevier Ltd. This is an open access article under the CC BY license (http://creativecommons.org/licenses/by/4.0/).

(*continued*)

HPECO	High-pressure economizer
HPEVA	High-pressure evaporator
HPSH	High-pressure super-heater
LHV	Lower heating value
LPECO	Low-pressure economizer
LPEVA	Low-pressure evaporator
LPSH	Low-pressure super-heater
m	Mass flow rate
n	Molar flow rate
P	Power generation
SHTR	Sensible heat thermochemical recuperation
ST	Steam turbine
SPECCA	Specific primary energy consumption for CO_2 avoided
η	Power generation efficiency of power plant
η_{ex}	Exergy efficiency of power plant
$\eta_{roundtrip}$	Roundtrip energy efficiency of the Power-to-NH_3-to-Power route

1. Introduction

Currently, natural gas combined cycle (NGCC) power generation accounts for more than 20 % of global power generation [1,2]. With the increasing share of intermittent and unstable renewable power sources, the future role of NGCC power plants remains crucial in balancing the supply and demand of energy systems. However, NGCC power plants are characterized by specific CO_2 emissions of about 350 kg/MWh, resulting in 7.1 Gt of CO_2 emissions in 2018 [3,4]. Therefore, decarbonizing NGCC power plants is essential to meet the target of limiting the temperature rise to 1.5 °C.

Among CO_2 mitigation technologies for NGCC power plants, CO_2 capture, utilization, and storage (CCUS) technology is crucial in net-zero emission transition scenarios. The CO_2 capture processes in NGCC power plants are divided into post-combustion, pre-combustion, and chemical looping combustion [5]. Compared with pre-combustion and chemical looping combustion, post-combustion CO_2 capture is the most suitable for existing NGCC power plants retrofitting due to advantages of requiring less modification [6]. According to CO_2 separation principles, CO_2 capture technologies employed in post-combustion configuration are mainly classified as chemical absorption, solid adsorption, and membrane technologies [7]. Among CO_2 separation technologies, high-temperature solid adsorption is recognized for its potential to achieve low-energy-consumption CO_2 capture since high-grade thermal energy can be recovered for power generation [8,9].

Calcium Looping (CaL) process has been extensively studied in previous research due to the wide availability and low cost of raw materials for solid adsorbents [10–13]. Depending on the location of the CaL process, two configurations are commonly used for post-combustion in NGCC power plants: hot-end and tail-end configurations [14]. In the hot-end configuration, CO_2 in the gas turbine exhaust gas is captured by the CaL process, and the decarbonized flue gas is then directed to the heat recovery steam generator (HRSG) unit. Retrofitting NGCC power plants with the hot-end CaL configuration results in energy penalties ranging from 5.0 % to 10.8 % [14–17]. On the other hand, in the tail-end CaL configuration, the CaL process is positioned behind the HRSG unit of existing NGCC power plants to capture CO_2 in the low-temperature flue gas. Implementing the tail-end CaL configuration for NGCC decarbonization leads to energy penalties ranging from 10.6 % to 12.0 % [14,18,19]. The tail-end CaL configuration can be directly integrated into existing NGCC power plants without modification, although it incurs a higher energy penalty compared to the hot-end CaL configuration.

In the benchmark tail-end CaL configuration, natural gas oxy-fuel combustion supplies heat for the endothermic calcination reaction. The need for high-purity oxygen results in significant energy consumption and high costs due to the air separation unit (ASU). The power consumption and installation cost of ASU represent over 40 % of the electricity demand of CaL system and approximately 15 % of the total plant cost, respectively [20–22]. To reduce ASU power consumption, different heating supply methods are proposed to replace oxy-fuel combustion including combination of calcium looping and chemical looping combustion [23–26], solar-driven calcination [27–31]. However, combing calcium looping and chemical looping combustion introduces additional CO_2 capture requirements due to the use of fossil fuel. In the solar-driven calcination process, the intermittent nature of solar energy necessitates solid reservoirs for CaO and $CaCO_3$ storage, limiting calcination to daytime operations.

This paper introduces a novel CaL process driven by carbon-free fuel ammonia (NH_3), eliminating CO_2 capture requirements from fossil fuel combustion for heating supply of calcination. To avoid the CO_2 emissions and fossil fuel consumption during NH_3 production, NH_3 produced from renewable energy (also known as green NH_3) is suggested as the feedstock. As a zero-carbon fuel and hydrogen carrier, NH_3 is gaining attention for its high energy density, easy storage and well-established infrastructure. Ammonia can be blended with coal or NG for heat and/or power generation, which have been successfully demonstrated [32–35]. However, ammonia combustion suffers a few challenges for direct combustion such as high ignition energy, low flame speed and potential fuel NOx [36,37]. One of the strategies is to partially crack ammonia using exhaust heat to produce ammonia/hydrogen mixture which is then injected into combustion chamber. The presence of hydrogen can enhance ammonia combustion. In the green NH_3-driven CaL process proposed, thermochemical recuperation of carbonation heat is recovered to crack NH_3 to both enhance the thermodynamic performance and enable effective combustion.

This study, to the best of our knowledge, is the first to focus on the integration of CaL for CO_2 capture and NH_3 combustion while recovering carbonation heat via NH_3 cracking. We will introduce two integration schemes for NGCC systems with tail-end CO_2 capture using the green NH_3-driven CaL method with carbonation heat chemical recuperation. A new criterion for evaluating energy consumption for CO_2 avoided will be introduced. Detailed energy analysis will illustrate the energy distribution differences among NGCC systems with tail-end CO_2 capture. Furthermore, exergy analysis and Energy Utilization Diagrams (EUDs) will reveal the energy-saving mechanisms, and sensitivity analysis on thermodynamic performance will be conducted. In addition, when green ammonia is produced from the excess renewable electricity, the equivalent roundtrip energy efficiency of the power-to-NH_3-to-power route is evaluated.

2. System description

2.1. Integration idea

Fig. 1 illustrates the integration concept of the novel green NH_3-driven calcium looping method with thermochemical recuperation. In this process, flue gas from fossil fuel-based power plants undergoes

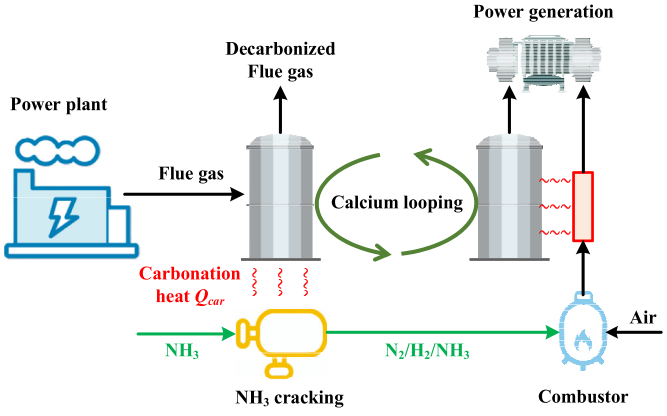


Fig. 1. The integration idea based on the novel green NH_3-driven CaL with thermochemical recuperation method.

decarbonization via the carbonation/calcination cycle. The exothermic carbonation process's heat is recovered by the NH_3 cracking process, while the endothermic calcination process's heat requirement is met by combusting the cracking products at high temperatures. The sensible heat from high-temperature streams is then directed to the power generation unit. Compared to the traditional CaL-Oxy method, the green NH_3-driven, chemically recuperated tail-end calcium looping method offers several advantages: (1) using carbon-free ammonia instead of fossil fuels for flue gas decarbonization eliminates the need for CO_2 capture from calcination energy donors. (2) the novel concept avoids the high energy consumption associated with producing high-purity oxygen and reduces the irreversibility caused by oxy-fuel combustion. (3) The mid-temperature carbonation heat can be converted into the chemical energy of H_2, which can be combusted and integrated with a combined cycle. The proposed green NH_3-driven calcium looping method with thermochemical recuperation is expected to enhance carbonation heat utilization efficiency and reduce the energy consumption of CO_2 capture.

2.2. Proposed systems with two schemes

Figs. 2 and 3 illustrate two integration system schematics for NGCC power plant decarbonization: the sensible heat thermochemical recuperation (SHTR) scheme and the carbonation heat thermochemical recuperation (CHTR) scheme, respectively. The NGCC power plant primarily comprises a gas turbine (GT) unit, a heat recovery steam generator (HRSG), and a steam turbine (ST). Natural gas and compressed air are combusted and then sent to drive the gas turbine to output work. The high-temperature exhaust gas at the turbine outlet enters the HRSG to heat steam for driving the steam turbine to perform work. The HRSG includes a high-pressure super-heater (HPSH), a high-pressure evaporator (HPEVA), a low-pressure super-heater (LPSH), a high-pressure economizer (HPECO), a low-pressure evaporator (LPEVA), a low-pressure economizer (LPECO) and a feedwater heater (FWH). In the SHTR scheme (Fig. 2), cooled flue gas from an NGCC power plant is sent to the carbonator, where CO_2 is absorbed. Due to the low CO_2 concentration and temperature of the flue gas, more heat is converted to the sensible heat of the inlet gas. The carbonator operates endothermically without the need for flue gas preheating. Thus, the sensible heat of the decarbonized flue gas is sequentially recovered for NH_3 cracking and preheating the flue gas following the carbonation process. In the cracker, NH_3 from the storage tank is compressed and decomposed with the aid of a catalyst. The cracking products are then mixed with compressed air and sent to the combustor. The carbonated solid $CaCO_3$ is conveyed to the calciner, where it regenerates CaO and releases CO_2. The heat demand of the calcination process is met by the sensible heat of high-temperature combustion products from the $NH_3/H_2/N_2$ combustor. After providing heat for the calcination process, the combustion products are expanded in the gas turbine. The sensible heat of the exhaust gas and CO_2 from the calciner is recovered in the HRSG2 unit. Additionally, the sorbent activity of CaO decreases over numerous carbonation/calcination cycles. Therefore, a small proportion of regenerated CaO is purged after calcination, and fresh $CaCO_3$ is added to maintain sorbent activity.

In contrast to the SHTR scheme, the CHTR scheme preheats the flue gas to a higher temperature, making the carbonator operate exothermically. As shown in Fig. 3, a thermally coupled shell-tube reactor, successfully demonstrated for methane chemical looping reforming, is used. In this reactor, NH_3 cracking occurs in catalyst-packed tubes located inside the carbonator, where carbonation heat is transferred to the tubes. After the carbonation and cracking processes, the cracking products are combusted, and the carbonation solids are decomposed to release CO_2. The subprocesses in the CHTR scheme are similar to those in the SHTR scheme. The sensible heat of the combustion products is recovered by the calcination process and the combined cycle, and the CO_2 from the calciner is directed to the HRSG2 unit for power

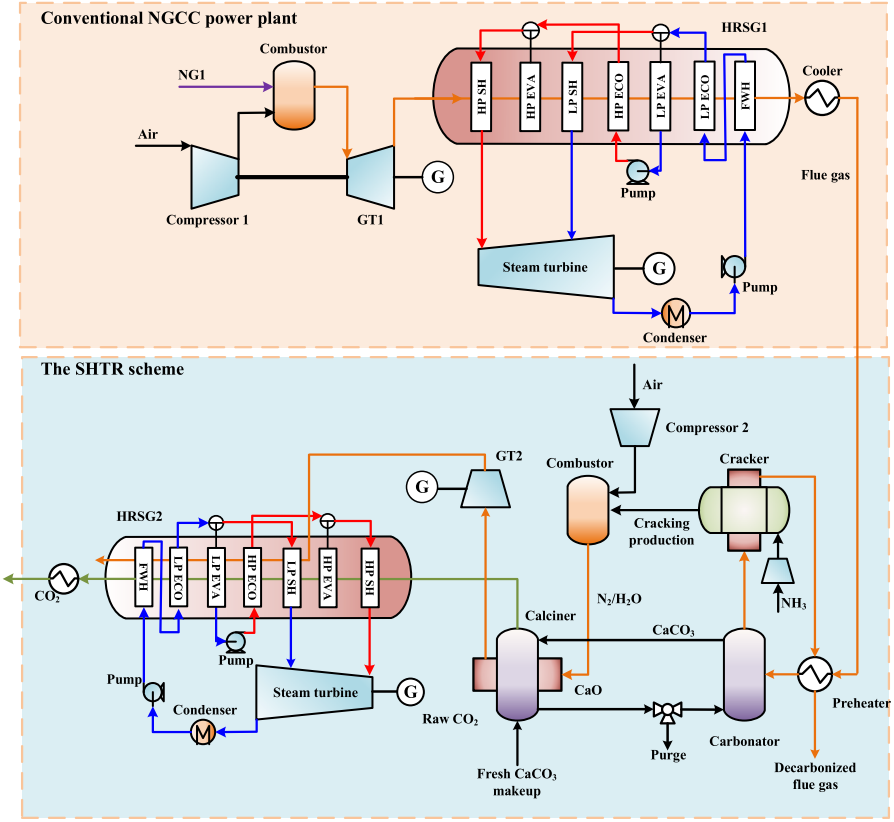


Fig. 2. Schematic of the proposed NGCC power plant with the SHTR scheme.

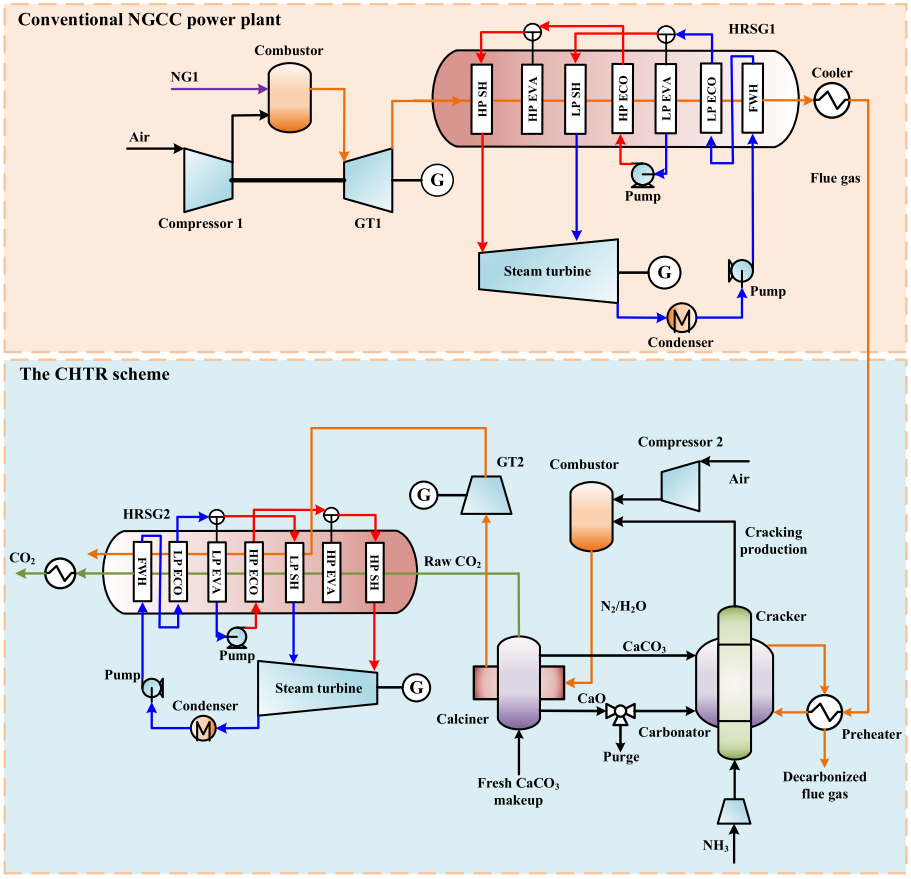


Fig. 3. Schematic of the proposed NGCC power plant with the CHTR scheme.

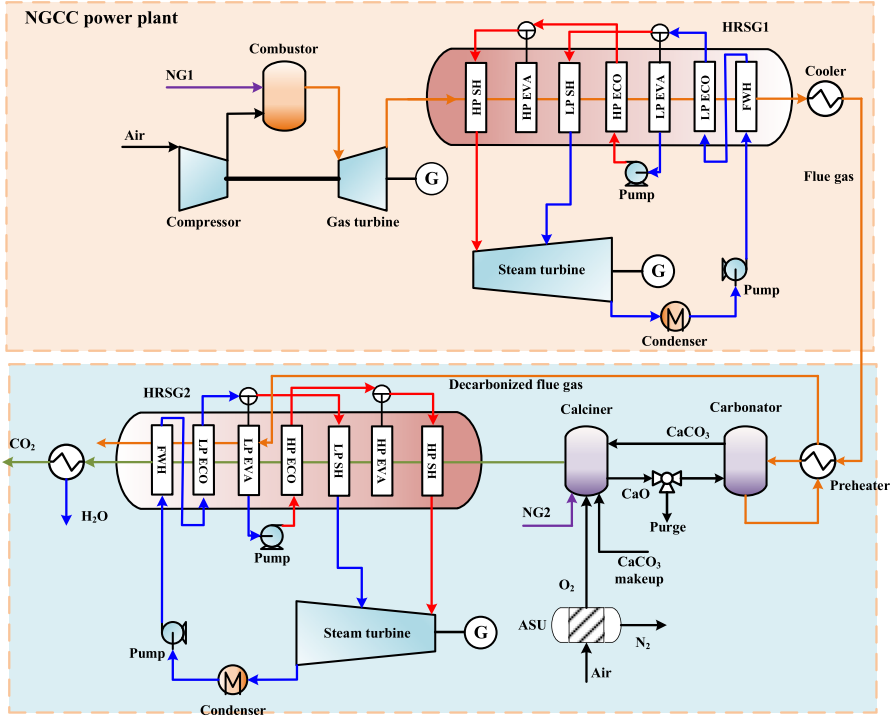


Fig. 4. Schematic of the reference NGCC system with tail-end CO_2 capture based on the CaL-Oxy method.

generation.

2.3. Reference system

To compare the plant-level thermodynamic performance, the NGCC power plant with tail-end CO_2 capture based on the CaL-Oxy method is selected as the reference system, with its schematic presented in Fig. 4. In this system, flue gas from the NGCC power plant is first preheated to maintain thermal balance in the carbonator. The carbonated sorbent, $CaCO_3$, is then sent to the calciner, where it decomposes into CaO and CO_2. In the CaL-Oxy configuration, natural gas oxy-fuel combustion supplies the heat required for calcination. High-purity oxygen from the ASU is mixed with natural gas and fed to the calciner. Following the carbonation/calcination cycle, the sensible heat from high-temperature gas production is recovered for power generation. With the carbonator and calciner operating at atmospheric pressure, the raw CO_2 (mainly consisting of CO_2 and H_2O) from the calciner, along with the decarbonized flue gas is directed to the HRSG2 unit instead of being directly expanded in the gas turbine.

2.4. System evaluation criteria

To evaluate the thermodynamic and economic performance of the proposed systems, some system evaluation criteria are introduced including CO_2 capture ratio (CCR), energy penalty, energy consumption for CO_2 avoided (EC_A).

As shown in Eq. (1), CCR is defined as the ratio between captured CO_2 amount and total carbon amount carried by natural gas and fresh $CaCO_3$ makeup solids.

$$CCR = \frac{n_{CO_2,captured}}{n_{CaCO_3,make-up} + n_{NG,input}} \tag{1}$$

where $n_{CO2,\ captured}$, $n_{CaCO3,\ make\text{-}up}$, and $n_{NG,\ input}$ represent the mole flow of CO_2 captured, fresh $CaCO_3$ makeup solids, and total natural gas input, respectively. In this study, the CCR for three systems is selected as 90 %.

For the proposed and reference systems, the detailed calculation of power generation efficiency is shown Eq. (2).

$$\eta_p = \frac{P_{GT} + P_{STs} - P_{Pumps} - P_{ASU} - P_{Comps} - P_{Solids}}{m_{NG}LHV_{NG} + m_{NH_3}LHV_{NH_3}} \tag{2}$$

where P_{GT}, P_{STs}, P_{Pumps}, P_{ASU}, P_{Comps} and P_{Solids} represent the power generation in gas turbines and steam turbines, and power consumption in pumps, ASU unit, compressors and solids conveying. Besides, m_{NG}, and m_{NH3} represent mass flow of natural gas input and NH_3 input in these systems, respectively. LHV_{NG}, and LHV_{NH3} are the lower heating value of natural gas input and NH_3 input, respectively.

Energy penalty represents the power generation efficiency reduction of power plants after equipping with CO_2 capture unit. The definition of energy penalty is depicted as Eq. (3) [38].

$$\Delta\eta = \eta_{wo} - \eta_w \tag{3}$$

where η_w and η_{wo} are the power generation efficiencies of the NGCC power plants with and without CO_2 capture, respectively.

Exergy efficiency is defined as the ratio between net power output and exergy input, as shown in Eq. (4).

$$\eta_{ex} = \frac{P_{net}}{EX_{in}} = \frac{P_{GT} + P_{STs} - P_{Pumps} - P_{ASU} - P_{Comps} - P_{Solids}}{m_{NG}Ex_{NG,ch} + m_{NH_3}Ex_{NH_3,ch}} \tag{4}$$

where P_{out} and EX_{in} are the net power output and exergy input of power systems, respectively. $Ex_{NG,ch}$, and $Ex_{NH3,ch}$ represent the chemical exergy of natural gas and NH_3 input at the basis of per kilogram, respectively.

Besides, detailed exergy destruction of subprocess in these systems are calculated according to exergy balance relationship (described in Eq. (5)).

$$EX_{in} = EX_{out} + EX_{des} + Q \cdot (1 - T_0 / T) + P_{out} \tag{5}$$

where EX_{in}, EX_{out}, $Q(1\text{-}T_0/T)$, and P_{out} are exergy input of streams, exergy output of streams, exergy of thermal energy output, power output, respectively. EX_{des} is the exergy destruction of the process.

EC_A depicts the extra equivalent energy consumption of CO_2 avoided at basis of mass unit. Given that there are two types of fuel input in the proposed system, the EC_A is defined as Eq. (6) where the equivalent energy consumption proportions are selected with the proposed system.

$$EC_A = 3600 \cdot \frac{\frac{P_{net,wo}}{P_{net,w}}(1/\eta_w - 1/\eta_{wo}) + \frac{(P_{net,w} - P_{net,wo})}{P_{net,w}}(1/\eta_w - 1/\eta_{NH_3})}{\frac{P_{net,wo}}{P_{net,w}}CE_{wo} + \frac{(P_{net,w} - P_{net,wo})}{P_{net,w}}CE_{NH_3} - CE_w} \tag{6}$$

where P_{net} and CE are the net power output and carbon emission intensity of NGCC power plants, respectively. η_{NH3} means the power generation efficiency of selected NH_3 based thermochemical recuperation power system, which operates with the identified gas turbine inlet temperature and pressure with that in the two thermochemical recuperation schemes. Since there is no NH_3 based thermochemical recuperation power plant operating in industrial scale, a typical NH_3 based thermochemical recuperation power system integrating with GT in previous study is selected to evaluate the EC_A of the proposed systems [39]. The schematic of the NH_3 based thermochemical recuperation power system is shown in Fig. A1, and power generation efficiencies under different gas turbine inlet temperature and pressure are illustrated in Fig. A2. The carbon emission intensity of selected NH_3 based thermochemical recuperation power system (CE_{NH3}) is 0 kg/MWh. The subscript w, and wo represent with and without CO_2 capture, respectively.

In the reference system based on the CaL-Oxy method, only natural gas is selected as fuel input. When η_{NH3} and CE_{NH3} are selected identical with η_{wo} and CE_{wo}, the EC_A in Eq. (6) can be simplified as Eq. (7), which is identified as the spesific energy consumption for CO_2 avoided in previous studies [40].

$$EC_A = 3600 \cdot \frac{(1/\eta_w - 1/\eta_{wo})}{CE_{wo} - CE_w} \tag{7}$$

3. Key process simulation and model validation

3.1. NH_3 cracking process

The NH_3 cracking reaction (shown in Eq. (8)) is an endothermic process occurring at relatively high temperatures, ranging from 350 to

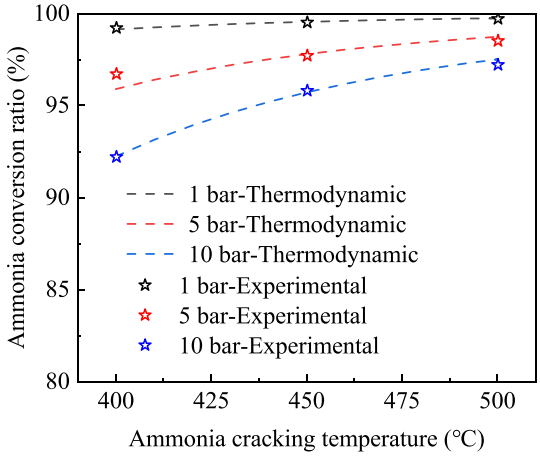


Fig. 5. Comparison of thermodynamic analysis results with experimental results [42].

900 °C [41]. In previous studies, an RGibbs reactor has been employed to simulate the NH_3 cracking process, and thermodynamic analysis has been conducted to calculate the equilibrium composition. Fig. 5 presents the thermodynamic analysis and experimental results of the NH_3 cracking process, operating at temperatures between 400 °C and 500 °C and pressures ranging from 1 bar to 10 bar using commercial Ru/Al_2O_3 catalysts [42]. The comparison between simulation and experimental results shows good agreement.

$$NH_3 = 0.5N_2 + 1.5H_2 \ \Delta H_{298K} = -46.2\ kJ/mol \quad (8)$$

3.2. Calcium looping subprocesses

During the calcium looping process, flue gas from the NGCC power plant is preheated and introduced to the carbonator, which operates at a temperature of 600–700 °C and atmospheric pressure. The absorption capacity depends on the average CaO conversion, so the carbonator is modeled using the Rstoic block [43,44]. Subsequently, the calcination of $CaCO_3$ (as shown in Eq. (10)) occurs in the calciner at 900 °C. In the CaL-Oxy method, natural gas and high-purity oxygen are sent to the calciner, where natural gas is combusted to supply the necessary heat for the calcination reaction. The main combustion reaction of natural gas is shown in Eq. (11). Both the calcination and oxy-fuel combustion reactions operate at high temperatures, allowing chemical equilibrium to be achieved. The calciner reactor is modeled using RGibbs reactors [45–47]. To simplify the model, the ASU unit in the CaL-Oxy method is treated as a black box, with energy consumption and oxygen purity values selected from the literature [48,49]. A typical flue gas decarbonization via the CaL-Oxy method is simulated and compared with the literature in Table 1. The simulation results show good agreement with previous studies.

$$CO_2 + CaO = CaCO_3 \ \Delta H_{298K} = -178.4\ kJ/mol \quad (9)$$

$$CaCO_3 = CaO + CO_2 \ \Delta H_{298K} = +178.4\ kJ/mol \quad (10)$$

$$CH_4 + 2O_2 = 2CO_2 + 2H_2O \ \Delta H_{298K} = -890.6\ kJ/mol \quad (11)$$

3.3. Power generation subprocesses

The power generation subprocesses include combustors, compressors, gas turbines, steam turbines, HRSG units, and water pumps. Compressor blocks are used to simulate the compressors, gas turbines, and steam turbines, while Pump blocks are employed to pressurize water in the Rankine cycle [50]. MheatX blocks simulate the heat exchanges in the HRSG unit, and the combustor is modeled using an RGibbs reactor [51]. In the two thermochemical recuperation schemes, the combustion process of the cracking products (main reactions shown in Eq. (12) and Eq. (13)) operates under adiabatic conditions. The outlet temperature is adjusted by the air excess ratio to meet the heat demand of the calcination process. Using this simulation method, the base NGCC power plant is modeled. The simulation results, as shown in Table 2, demonstrate the reliability of the power generation models.

$$2H_2 + O_2 = 2H_2O \ \Delta H_{298K} = -571.6\ kJ/mol \quad (12)$$

$$2NH_3 + 1.5O_2 = N_2 + 3H_2O \ \Delta H_{298K} = -765.6\ kJ/mol \quad (13)$$

Table 1
Validation of the CaL-Oxy simulation.

Item	Literature [43]	Simulation
Carbonator operating temperature (°C)	650	650
Calciner operating temperature (°C)	900	900
Carbonator capture efficiency (%)	85	85
Fuel consumption (MW)	213.9	215.0
CO_2 captured from flue gas (kg/s)	27.2	27.2
CO_2 purity (%)	97.1	96.6

Table 2
Validation of power generation model.

Item	Industrial power plant [26]	Simulation
Natural gas input (kg/s)	7.42	7.42
Gas turbine inlet temperature (°C)	1100	1100
Compressor outlet pressure (bar)	12	12
Main steam temperature (°C)	527	527
Steam pressure (bar)	56/6.6	56/6.6
Condense pressure (bar)	0.097	0.097
Flow rate of feedwater (t/h)	212.0	212.0
Flue gas temperature (°C)	100	100
Net power output (MW)	180	187.9

3.4. Feedstocks and main operating parameters

For the proposed and reference systems, a base NGCC power plant with 2 × 180 MW units, located in Dongguan, China, is selected for CO_2 capture retrofitting. These NGCC power plants with CO_2 capture are simulated using Aspen Plus v11.0, with the PR-BM method chosen for global property calculations. In the calcium looping process, fresh make-up solids and ammonia input are simplified as $CaCO_3$ and NH_3, respectively. Calcium solids is conveyed by the mature pneumatic technology with a specific electricity consumption of approximately 10 kJ/(kg·100m) [52]. The main operating parameters in the two proposed systems and the reference system are listed in Table 3.

Table 3
Main operating parameters in the proposed and reference systems.

Items	Description
Feedstocks	
Natural gas input	Molar fraction: CH_4 (91.1 %), C_2H_6 (6.0 %), C_3H_8 (2.14 %), C_4H_{10} (0.66 %), N_2 (0.05 %), CO_2 (0.04 %), O_2 (0.01); Lower heating value (LHV): 49.44 MJ/kg; Temperature and pressure of natural gas input: 25 °C and 24.7 bar [26].
NH_3 input	100 % NH_3; LHV: 18.50 MJ/kg; Temperature and pressure of natural gas input: 4 °C and 1.013 bar [53].
Solid make up	100 % $CaCO_3$; Temperature of fresh make-up solids: 25 °C, make-up ratio: 2.0 % [27,54].
Base NGCC power plant [26]	
Air compression	Outlet pressure: 12 bar; Isentropic efficiency: 0.85.
Gas turbine	Inlet temperature: 1100 °C; Isentropic efficiency: 0.92.
HRSG	Double-pressure without reheat steam; Pressure of steam: 56/6.5 bar; Steam temperature: 527 °C; Isentropic efficiency of steam turbines: 0.89/0.87; Condense pressure: 0.097 bar; Outlet temperature of HRSG: 100 °C.
Flue gas	Temperature of flue gas treated: 40 °C.
CaL units	
Carbonator	Carbonator pressure: 1.013 bar; Carbonator temperature: 600 °C [15,17]; Average CaO conversion: 0.2 [43,44]; Inlet temperature in the CaL-Oxy method and SHTR scheme: 370 °C; Inlet temperature in the CHTR scheme: 525 °C.
Calciner	Calcination temperature: 900 °C; Pressure: 1.013 bar.
HRSG2	Same with HRSG in the base NGCC power plant.
ASU	Cryogenic distillation technology; Electricity consumption: 180 kWh/t O_2; Purity of O_2: 95 % [48,49].
Solids conveying	Specific electricity consumption of solids conveying: 10 kJ/(kg·100m); Carbonator to calciner distance: 100 m [52].
Other processes in in thermochemical recuperation method	
Ammonia cracking	Cracking temperature: 400 °C; Cracking pressure: 6–21 bar [39]; Minimum temperature difference between decarbonized flue gas outlet and cracking temperature in SHTR method: 20 °C [55].
Gas turbine	Inlet temperature: 1000–1200 °C [39]; Exhaust pressure: 1.013 bar; Isentropic efficiency of GT: 0.92.
Air compressor	Isentropic efficiency: 0.85.
Cracking production combustor	Adiabatic.

4. Results and discussion

4.1. Energy analysis

To accurately compare energy distributions, the gas turbine inlet temperature and pressure are set to 1100 °C and 12 bar, consistent with those in the base NGCC power plant. Detailed energy analysis is provided in Table 4. The two proposed systems demonstrate superior thermodynamic performance compared to the NGCC power plant using the CaL-Oxy method. Specifically, the power generation efficiencies are 49.4 % for the SHTR scheme and 49.9 % for the CHTR scheme, resulting in energy penalties of 1.8 % and 1.4 %, respectively.

The difference in energy penalty is attributed to the integration of the calcium looping process with chemical energy conversion. Since the enthalpy change of NH_3 cracking is lower than that of the carbonation reaction, the two thermochemical recuperation schemes require more chemical energy input. However, this chemical energy is effectively recovered and converted into power, reducing the energy penalty. In the SHTR scheme, the chemical energy input in the CaL unit is 401.6 MW, resulting in a power output increase of 192.0 MW. In the CHTR scheme, the input is 425.9 MW, leading to a 205.4 MW increase in power output. In contrast, the NGCC power plant using the CaL-Oxy method sees only a 22.9 MW increase in power output with a 139.2 MW chemical energy input due to inefficient heat recovery and additional ASU power consumption. In the two thermochemical recuperation schemes, part of the carbonation heat is recovered and converted into the chemical energy of cracking products. This chemical energy is then transformed into high-grade thermal energy for the calcination process and recovered for power generation via the combined cycle. In the CaL-Oxy method, chemical energy is directly combusted to supply heat for calcination, and high-grade thermal energy is recovered through the Rankine cycle in the HRSG unit. Thus, the efficient use of NH_3 in the combined cycle improves power generation and eliminates ASU power consumption, leading to a reduced energy penalty in the two proposed NGCC power plants.

Table 4
The results of energy analysis.

Items	NGCC-base plant	Proposed NGCC		NGCC with CaL-Oxy method
		SHTR scheme	CHTR scheme	
Energy input				
NG-base (MW)	366.7	366.7	366.7	366.7
NG-CaL (MW)	0	0	0	139.2
NH_3-CaL (MW)	0	401.6	425.8	0
Total energy input (MW)	366.7	768.3	792.5	505.9
Energy output				
GT-base (MW)	270.9	270.9	270.9	270.9
Compressors-base (MW)	−147.7	−147.7	−147.7	−147.7
GT-CaL (MW)	0	268.6	291.4	0
Compressors-CaL (MW)	0	−139.2	−151.4	0
STs-base (MW)	65.2	65.2	65.2	65.2
STs-CaL (MW)	0	65.5	70.3	33.6
Pumps-base (MW)	0.5	−0.5	−0.5	−0.5
Pumps-CaL (MW)	0	−0.4	−0.5	−0.2
Solids conveying-CaL (MW)	0	−2.5	−2.5	−2.4
ASU in CaL-Oxy (MW)	0	0	0	−8.1
Net power output (MW)	187.9	379.8	395.3	210.8
Power generation efficiency (%)	51.2	49.4	49.9	41.7
Energy penalty (%)	–	1.8	1.4	9.6
CE (kg CO_2/MWh_e)	392.6	21.1	20.3	51.3
EC_A (MJ_{LHV}/kg CO_2)	–	−5.44	−6.33	4.73

The use of zero-carbon fuel in the CaL unit enhances green power penetration, leading to a reduction in carbon emission intensity. For a CO_2 capture ratio of 90 %, the carbon emission intensities of the two proposed NGCC power plants are 21.1 kg CO_2/MWh_e and 20.3 kg CO_2/MWh_e, respectively, which are lower than that of the NGCC power plant using the CaL-Oxy method (51.3 kg CO_2/MWh_e). Additionally, the efficient use of NH_3 for power generation further reduces the EC_A in the proposed systems. The NH_3 thermochemical recuperation power plant achieves a power generation efficiency of 38.3 %, largely due to high exhaust gas temperatures exceeding 300 °C [39]. This results in primary energy savings of 5.44 MJ_{LHV}/kg CO_2 in the SHTR scheme and 6.33 MJ_{LHV}/kg CO_2 in the CHTR scheme. In contrast, the NGCC power plant with the CaL-Oxy method has a EC_A of 4.73 MJ_{LHV}/kg CO_2 due to less efficient energy conversion and higher energy consumption for CO_2 avoidance. The CaL-Oxy method uses thermal energy from natural gas through the Rankine cycle, whereas the base power plant employs a combined cycle. In summary, integrating NH_3 utilization with the calcium looping process not only improves the efficiency of NH_3 chemical energy use but also enhances high-grade heat recovery, leading to greater primary energy savings for CO_2 avoided compared to both the NGCC base power plant and the NH_3 thermochemical recuperation power plant.

4.2. Exergy destruction distributions comparison

Fig. 6 illustrates the exergy destruction distribution across subprocesses in three NGCC systems with tail-end CO_2 capture. For the two proposed NGCC power plants using the thermochemical recuperation method, exergy efficiencies are 46.9 % for the SHTR scheme and 47.3 % for the CHTR scheme. These efficiencies represent an improvement of 6.7 percentage points in the SHTR scheme and 7.2 percentage points in the CHTR scheme compared to the NGCC power plants using the CaL-Oxy method.

In the two proposed systems, the NGCC base power plant experience reduced exergy destruction compared to that in the reference system, due to increased chemical energy penetration. This results in a reduction of exergy destruction by 12.2 percentage points in the SHTR scheme and 12.9 percentage points in the CHTR scheme compared to the NGCC power plant with the CaL-Oxy method. The exergy destruction in the carbonator is similar between the NGCC power plant using the SHTR scheme and the CaL-Oxy method. However, the increased chemical energy in the SHTR scheme leads to a reduced proportion of exergy destruction. In contrast, the carbonator in the NGCC power plant with the CHTR scheme benefits from a higher inlet temperature, further reducing exergy destruction.

When comparing exergy destruction in preheaters, the sensible heat from outlet decarbonized flue gas is directly recovered in both the CaL-Oxy method and the CHTR scheme. This direct recovery leads to an exergy destruction proportion ranging from 5.7 % in the CaL-Oxy method to 1.6 % in the CHTR scheme. In the SHTR scheme, high-temperature sensible heat is first recovered through the NH_3 cracking process, with low-temperature sensible heat recovered through preheating flue gas. This cascaded heat recovery approach results in a 1.1 percentage point reduction in exergy destruction in the preheater compared to the CHTR scheme. Overall, recovering carbonation heat and high-temperature sensible heat of decarbonized flue gas results in 2.1 % and 1.8 % exergy destruction in the two schemes, respectively. The difference in exergy destruction for NH_3 cracking is influenced by the amount of NH_3 input, which is determined by the heat recovered in each scheme.

Different heating supply methods lead to variations in exergy destruction during the calcination process. In the CaL-Oxy method, oxy-fuel combustion results in 1.1 % exergy destruction in the ASU unit and 8.9 % in the calcination process. In contrast, the thermochemical recuperation methods replace oxy-fuel combustion with high-temperature heat recovery from combustion production. This substitution

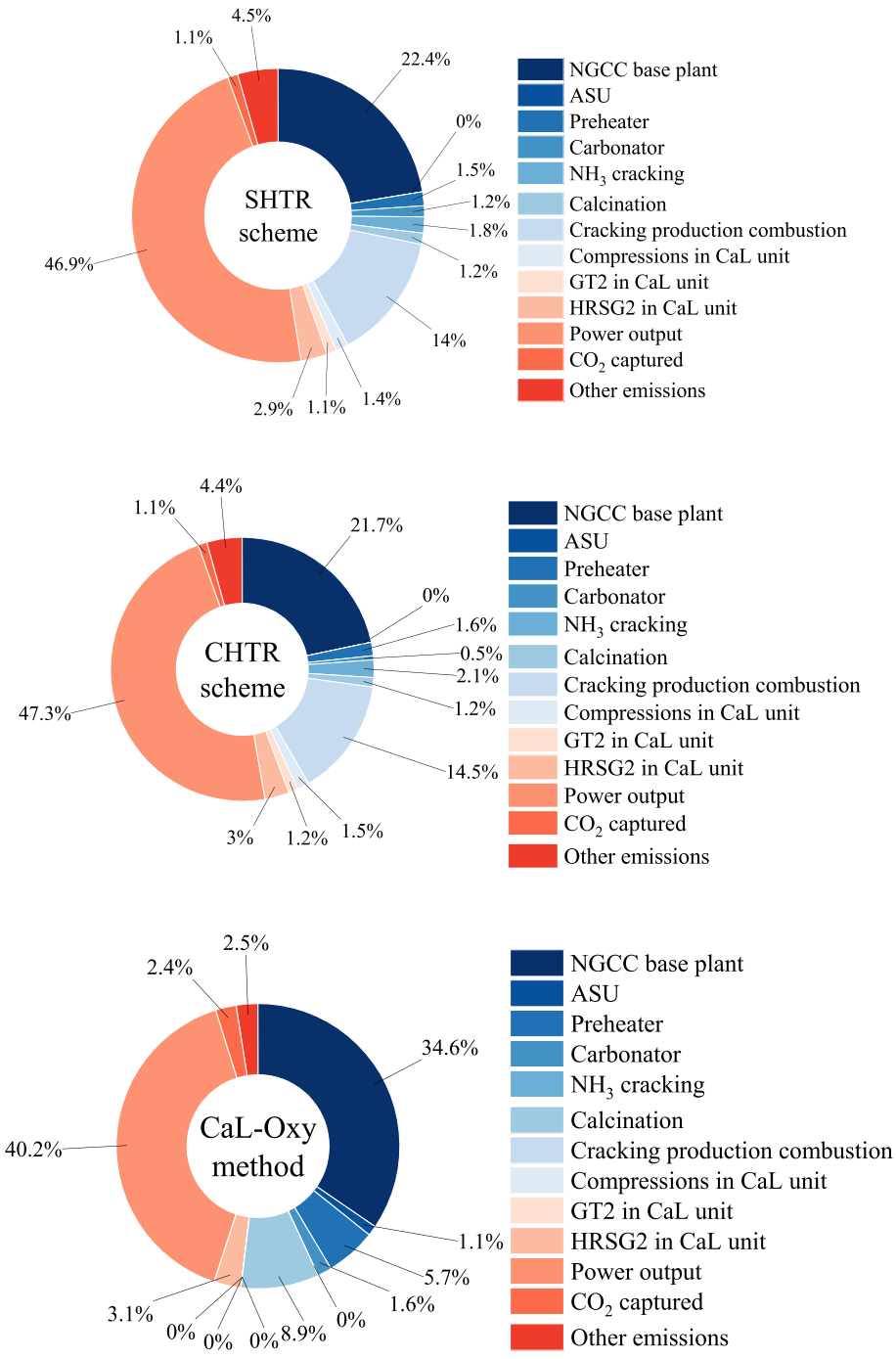


Fig. 6. Exergy destruction distributions in three NGCC power plants with tail-end CO_2 capture.

eliminates exergy destruction in both the ASU unit and fuel combustion. As a result, the exergy destruction in the calcination process is reduced by 7.7 percentage points in both thermochemical recuperation schemes.

The difference in exergy destruction among the three systems is influenced by both the carbonation and calcination processes, as well as heat integration methods. In the NGCC power plant with the CaL-Oxy method, the calciner operates at atmospheric pressure, and the sensible heat from raw production is recovered by the HRSG unit. In the thermochemical recuperation schemes, cracked ammonia is combusted, and the high-temperature sensible heat is recovered through a combined cycle after providing heat for the calcination process. This approach increases chemical energy input and adds exergy destruction in the cracking production combustion process, gas turbines, and compressors. Specifically, additional exergy destruction increases by 16.4 % in the SHTR scheme and 17.1 % in the CHTR scheme. Despite this, the use of a combined cycle enhances power generation. Accounting for the reduction in exergy destruction compared to the NGCC base power plant, the total exergy destruction increases by 4.7 percentage points in the SHTR scheme and 4.2 percentage points in the CHTR scheme.

In summary, the total reduction in exergy destruction due to the carbonation and calcination processes is 10.5 percentage points in the SHTR scheme and 10.8 percentage points in the CHTR scheme. Although the thermochemical recuperation method leads to increased exergy destruction from additional chemical energy conversion for power generation, the reduction in exergy destruction from carbonation and calcination outweighs this increase. Consequently, both

thermochemical recuperation schemes achieve enhanced power output.

4.3. Energy utilization diagrams in the carbonation process and calcination process

The reduction in exergy destruction during the carbonation and calcination processes enhances thermodynamic performance. The Energy Utilization Diagram (EUD) method further illustrates the mechanism of energy conversion [56–58]. In this method, energy is transferred from donors to acceptors, with energy level defined as the ratio of exergy change to enthalpy exchange (Eq. (14)). The difference in energy levels and exchanges between donors and acceptors contributes to process exergy destruction (Eq. (15)). Using the A-ΔH coordinate, the exergy destruction is represented by the area between the energy levels of donors and acceptors.

$$A = \Delta E / \Delta H \tag{14}$$

$$EX_{des} = \int (A_{ed} - A_{ea}) \cdot dH \tag{15}$$

Where ΔH is the enthalpy exchange between donors and acceptors, and A_{ed} and A_{ea} are energy level of donors and acceptors, respectively.

Fig. 7 presents the energy utilization diagrams of carbonation process among three NGCC power plant with the tail-end CO_2 capture. In the carbonation process of CaL-Oxy method, energy donors include solids CaO sensible heat releasing (A_{CaO}) and carbonation heat ($A_{carbonation\ heat}$) in the carbonator, and sensible heat releasing of decarbonized flue gas ($A_{Decarbonized\ flue\ gas}$) in the preheater. Flue gas preheating in the preheater ($A_{Flue\ gas\ preheating}$) and flue gas heating ($A_{Flue\ gas\ heating}$) in the carbonator play the role of energy acceptors. In the SHTR scheme and CHTR scheme, since carbonation heat and high-grade sensible heat of decarbonized flue gas are recovered to drive NH_3 cracking process. NH_3 preheating ($A_{NH3\ preheating}$) and NH_3 cracking reaction ($A_{NH3\ cracking}$) are included as energy acceptors. Comparing the EUD diagrams for the carbonation process in the SHTR scheme and the CaL-Oxy method, minimal differences are found in exergy destruction due to identical inlet flue gas temperatures and solids inventory in the carbonator. However, in the SHTR scheme, recovering high-grade sensible heat from decarbonized flue gas via NH_3 cracking reduces the energy level difference and thus lowers exergy destruction in the preheater. This results in a lower outlet temperature, indicating more effective recovery of sensible heat in the SHTR scheme. In the CHTR scheme, the reduction in both outlet temperature and energy level difference further decreases exergy destruction. Thus, extensive and cascaded sensible heat recovery in the preheater significantly contributes to reduced exergy destruction in the carbonation process across both thermochemical recuperation schemes.

Fig. 8 illustrates the energy utilization diagrams of calcination process among three NGCC power plants with the tail-end CO_2 capture. In the calcination process of the NGCC power plant with CaL-Oxy method, natural gas combustion process ($A_{combustion\ reaction}$) plays the role of the energy donor, and energy acceptors include fresh make-up solids heating process ($A_{make\text{-}up}$), carbonation solids heating process (A_{CaCO3}), O_2 heating process (A_{O2}), natural gas heating process (A_{NG}), and calcination reaction process ($A_{calcination}$). The exergy destruction in the calcination process primarily arises from natural gas combustion, which has a significantly higher energy level than the energy acceptors. In the two thermochemical recuperation schemes, natural gas combustion for heating is replaced by recovering sensible heat from combustion products. This change reduces the energy level difference between donors and acceptors. In both the SHTR and CHTR schemes, the average energy level of the recovered sensible heat from combustion products is approximately 0.8, compared to nearly 1.0 for natural gas combustion in the CaL-Oxy method. Additionally, this approach avoids the exergy

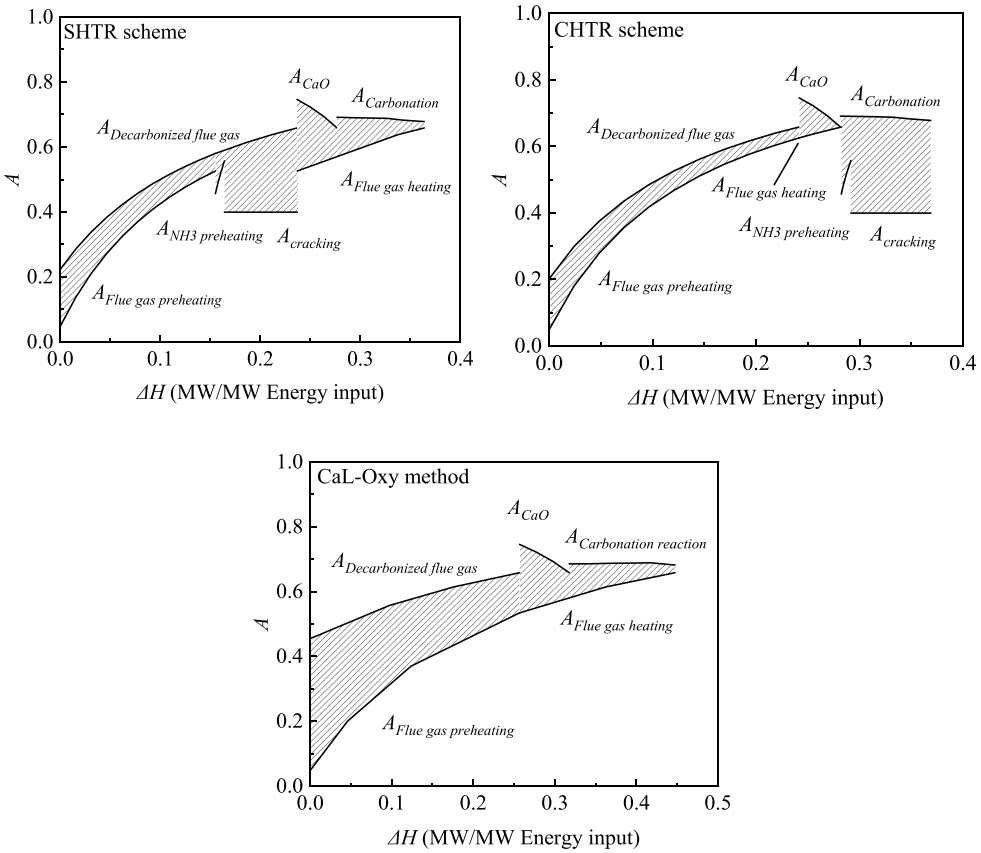


Fig. 7. Energy utilization diagrams of carbonation process among three systems.

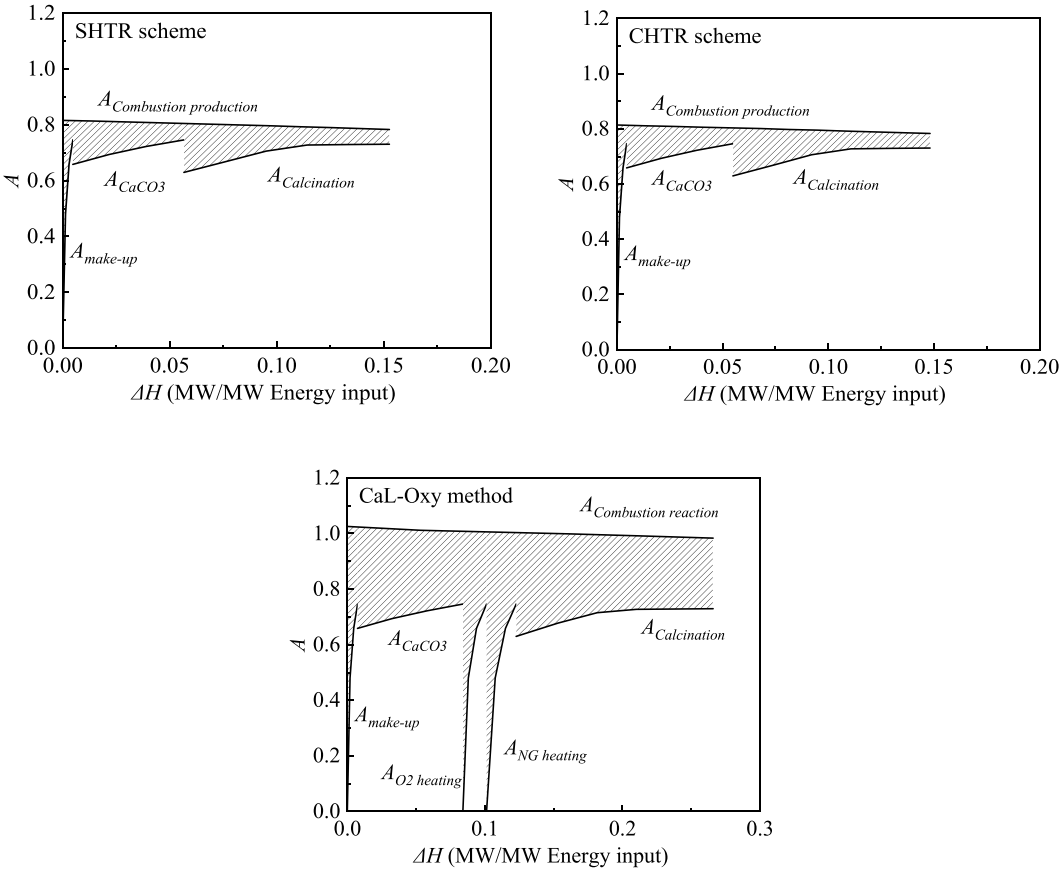


Fig. 8. Energy utilization diagrams of calcination process among three systems.

destruction associated with heating natural gas and oxygen.

4.4. Sensitivity analysis on thermodynamic performances in the two schemes

Fig. 9 illustrates the impact of gas turbine inlet temperature and pressure on the thermodynamic performance of the NGCC power plant with the CHTR scheme. As shown in Fig. 9 (a), increasing the gas turbine inlet temperature from 1000 °C to 1200 °C raises the outlet temperature of the cracking production combustor from 1145 °C to 1545 °C. Higher cracking pressure reduces the NH_3 conversion ratio, requiring more NH_3 to recover carbonation heat, which in turn decreases the outlet temperature due to the increased sensible heat carried by the combustion products. Fig. 9 (b) demonstrates that increasing the gas turbine inlet temperature enhances power generation efficiency. For instance, at a cracking pressure of 12 bar, efficiency rises from 49.5 % to 50.1 % as the gas turbine inlet temperature increases from 1000 °C to 1200 °C. Above 1100 °C, increasing cracking pressure improves efficiency, though the rate of improvement diminishes. Below 1100 °C, efficiency initially increases and then decreases with rising cracking pressure, indicating an optimal pressure for efficiency based on the isentropic efficiency of compressors and the gas turbine. Fig. 9 (c) shows that energy penalty follows a similar trend. When operating at a gas turbine inlet temperature of 1200 °C and a pressure of 21 bar, the NGCC power plant with the CHTR scheme achieves a power generation that surpasses the NGCC base power plant, resulting in an energy penalty reduction of −0.6 %. This negative energy penalty is due to the enhanced efficiency of the combined cycle in the CaL looping process, which compensates for the energy consumption of CO_2 capture, leading to overall energy savings.

Unlike power generation efficiency and energy penalty, increasing the gas turbine inlet temperature leads to a decline in EC_A. The minimum absolute value of EC_A is achieved at an optimal pressure when the NGCC power plant with the CHTR scheme operates with a gas turbine inlet temperature ranging from 1000 °C to 1200 °C. The greatest energy saving effect is observed at a gas turbine inlet temperature of 1000 °C and a pressure of 6 bar, where the NH_3 thermochemical recuperation power plant exhibits the lowest power generation efficiency under these conditions. Thus, the energy saving effect is influenced by both the thermodynamic performance of the NH_3 thermochemical recuperation power plant and the proposed NGCC power plant.

Fig. 10 illustrates the impact of gas turbine inlet temperature and pressure on the thermodynamic performance of the proposed NGCC power plant with the SHTR scheme. As the NH_3 input in the SHTR scheme is comparable to that in the CHTR scheme, a similar outlet temperature is required to meet the heat demand of calcination process. As shown in Fig. 10 (a), increasing the gas turbine inlet temperature from 1000 °C to 1200 °C raises the outlet temperature of the cracked NH_3 combustor from 1156 °C to 1540 °C. Fig. 10 (b) and Fig. 10 (c) reveal that, for gas turbine inlet temperatures between 1000 °C and 1200 °C and pressures ranging from 6 to 21 bar, the power generation efficiencies in the SHTR scheme range from 47.0 % to 51.3 %, while energy penalties range from 4.2 % to −0.1 %. Energy savings per kg of CO_2 avoided range from 4.99 MJ_{LHV} to 7.68 MJ_{LHV} (Fig. 10 (d)). The optimal energy saving is observed at a gas turbine inlet temperature of 1000 °C and a pressure of 6 bar.

4.5. Contribution to excess renewable electricity storage

NH_3 production consumes energy. In order to understand the influence of the energy required for NH_3 production, two NH_3 production methods were considered: (1) NG-based NH_3 production with carbon capture (known as blue NH_3) and (2) NH_3 production through renewable energy and green hydrogen (known as green NH_3).The typical case of proposed system with the SHTR scheme in Table 1 is selected to

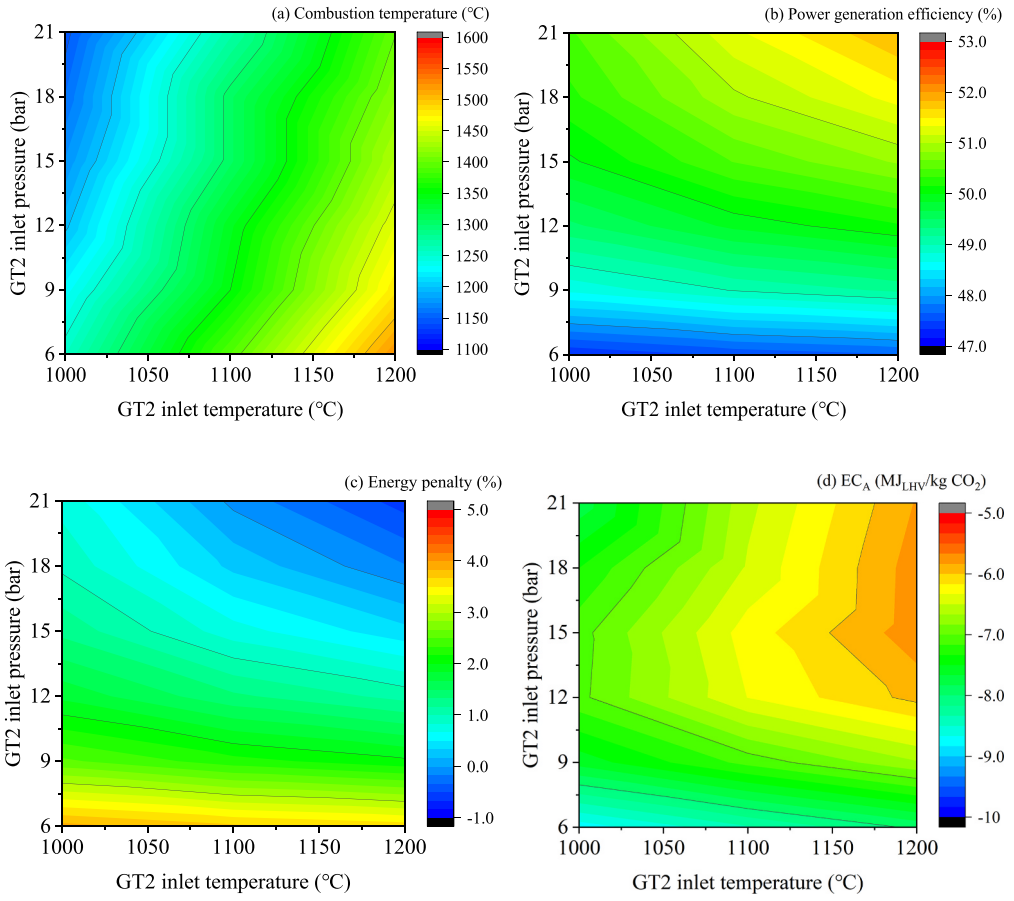


Fig. 9. Influence of gas turbine temperature and pressure on thermodynamic performances of proposed NGCC power plant in the CHTR scheme.

compare the overall energy efficiency, which is defined as the ratio between power output and fossil fuel input including fossil fuel consumed for NH_3 production. For the blue NH_3 production with an energy efficiency of 55.9 % [59], ignoring the energy consumption for NH_3 transportation, the natural gas consumption is 718.5 MW for the proposed SHTR scheme in Table 1. Therefore, considering NH_3 production in the SHTR system, the total natural gas input and power output are 1085.2 MW and 379.8 MW, respectively. As a result, the overall energy efficiency is 35.2 %, which is lower than that in the NGCC power plant with the CaL-Oxy method. This suggests that the energy loss during NG-based NH_3 production process offsets the energy saving during CO_2 capture process.

To avoid the fossil fuel energy consumption during NH_3 production process, green NH_3 from excess renewable electricity is suggested as the feedstock of the proposed NGCC decarbonization systems. Here green NH_3 acts as an energy storage media during the Power-to-X-to-Power roundtrip. When green NH_3 produced from excess renewable electricity is used, the proposed green NH_3-driven CaL process will both contribute to the NGCC power plant decarbonization and excess renewable electricity storage. To evaluate the renewable electricity storage effect of the NGCC systems with green NH_3-driven CaL process, the equivalent roundtrip energy efficiency is introduced taking the NGCC system with the CaL-Oxy as a reference. Discarding the energy consumption during NH_3 transportation the definition of the equivalent roundtrip energy efficiency is shown in Eq. (16) [60].

$$\eta_{eq,roundtrip} = \frac{P_{net} - E_{NG}\eta_{CaL-Oxy}}{E_{NH3}} \frac{E_{NH3}}{E_{\mathrm{Re}}} \tag{16}$$

where E_{NG} and $\eta_{CaL\text{-}Oxy}$ are the natural gas energy input in the proposed NGCC system with green NH_3-driven CaL process, and the power generation efficiency of the reference NGCC system with the CaL-Oxy method. Therefore, the two items in Eq. (16) represent the equivalent energy efficiency of green NH_3-to-power and renewable power-to-NH_3, respectively. The energy efficiency of the renewable power-to-NH_3 is 55.3 % when hydrogen production via electrolysis is selected as the feedstock of Haber-Bosch process [59].

For the direct NH_3-to-power process, the roundtrip energy efficiency of power-to-NH_3-to-power is defined in Eq. (17) [60].

$$\eta_{roundtrip} = \frac{P_{net-\mathrm{NH3}}}{E_{NH3}} \frac{E_{NH3}}{E_{\mathrm{Re}}} \tag{17}$$

where the first term represents the green NH_3-to-power efficiency of the NH_3-based thermochemical recuperation power plant.

For the NH_3-based thermochemical recuperation power plant, the NH_3-to-power efficiency ranges from 30.8 % to 42.8 % [39]. Based on Eq. (17), the roundtrip energy efficiency ranges from 17.0 % to 23.7 % for the direct NH_3-to-power route. When the green NH_3 is used for NGCC system decarbonization with the NH_3-driven CaL process, the equivalent roundtrip energy efficiency based on the NGCC systems with green NH_3-driven CaL process range from 28.9 % to 32.7 % in the SHTR scheme, and 29.3 %–32.9 % in the CHTR scheme, which is much higher than the roundtrip energy efficiency in the direct NH_3-to-power route. The enhancement of the energy efficiency indicates that the green NH_3-driven CaL process can not only reduce the energy consumption of CO_2 capture, but also be beneficial for excess renewable electricity storage.

5. Conclusions

This work proposes a novel concept of the green NH_3-driven calcium

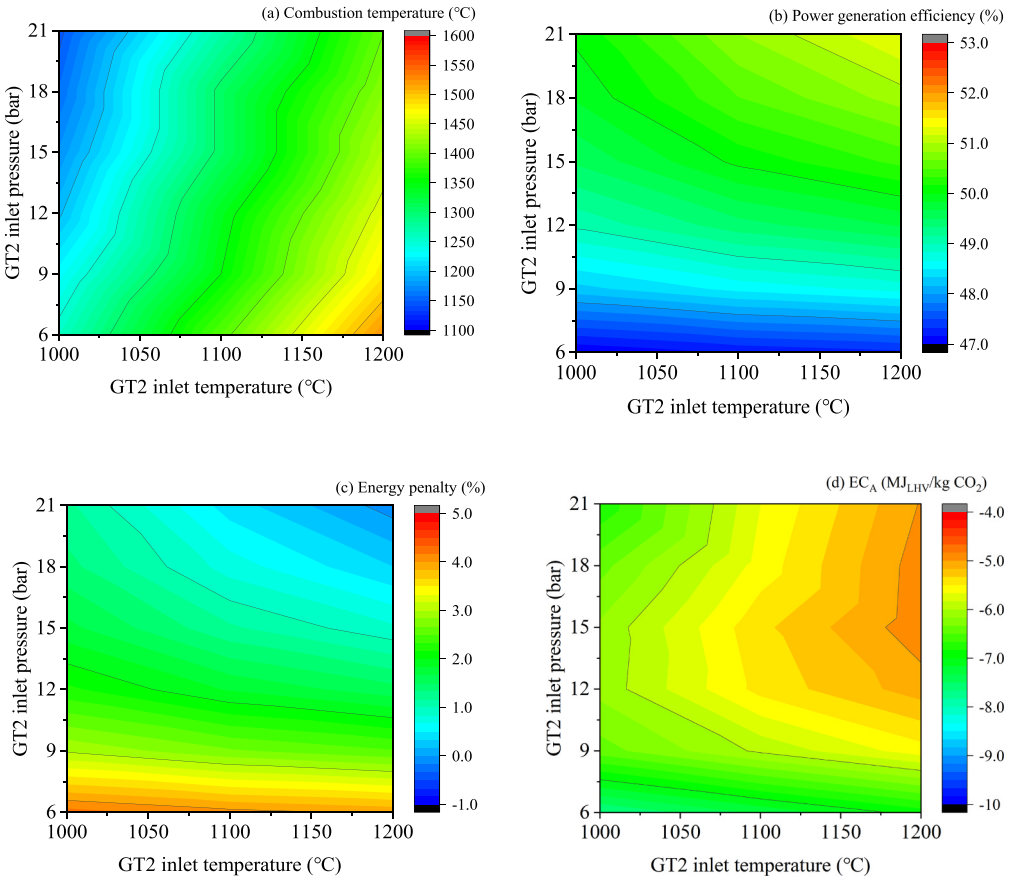


Fig. 10. Influence of gas turbine temperature and pressure on thermodynamic performances of proposed NGCC power plant in the SHTR scheme.

looping (CaL) process with thermochemical recuperation method, and two tail-end CO_2 capture integration schemes are introduced to decarbonize the natural gas combined cycle (NGCC) power plant. Besides, system evaluation, energy-saving mechanism and sensitivity analysis are investigated. Some conclusions can be drawn as follows.

(1) The power generation efficiencies are 49.4 % for the sensible heat thermochemical recuperation (SHTR) scheme and 49.9 % for the carbonation heat thermochemical recuperation (CHTR) scheme, resulting in energy penalties of 1.8 % and 1.4 %, respectively. The integration of NH_3 with a combined cycle enhances power generation and avoids additional air separation power consumption, leading to reduced energy penalties. Comparing with the NGCC base power plant and NH_3 thermochemical recuperation power plant, energy savings can be achieved at 5.44 MJ_{LHV}/kg CO_2 in the SHTR scheme and 6.33 MJ_{LHV}/kg CO_2 in the CHTR scheme.

(2) Comparing exergy destruction distributions of subprocesses among proposed and reference systems, it can be concluded that the exergy destruction reduction in carbonation and calcination process determines the thermodynamic enhancement. The total exergy destruction reduction caused by carbonation and calcination process is 10.5 percentage points in the SHTR scheme, and 10.8 percentage points in the CHTR scheme, respectively. Deep and cascaded heat recovery of carbonation heat narrows energy level difference in preheater and carbonator, lead to the exergy destruction reduction of carbonation process. For the calcination process, heating supply methods replacement avoids considerable exergy destruction caused by fuel-oxy combustion.

(3) Influences of gas turbine inlet temperature and pressure on energy penalties and EC_A are studied. When the two proposed NGCC power plant operate with gas turbine inlet temperature of 1200 °C and pressure of 21 bar, minus energy penalties can be achieved at −0.6 % in the CHTR scheme and 0.1 % in the SHTR scheme. This indicates that reorganizing more efficient thermodynamic cycle can cover the energy consumption of CO_2 capture from flue gas, resulting to the minus energy penalty. Besides, the optimum energy saving effect takes place under conditions with gas turbine inlet temperature of 1000 °C and pressure of 6 bar due to the power generation efficiency reduction of the NH_3 thermochemical recuperation power plant.

(4) When the green NH_3 is used for NGCC system decarbonization with the NH_3-driven CaL process, the roundtrip energy efficiency of power-to-NH_3-to-power is enhanced compared with the direct NH_3-to-power route. The roundtrip energy efficiencies range from 28.9 % to 32.7 % in the SHTR scheme, and 29.3 %–32.9 % in the CHTR scheme, respectively.

CRediT authorship contribution statement

Song He: Writing – original draft, Visualization, Validation, Methodology, Formal analysis, Data curation. **Xuelan Zeng:** Writing – review & editing, Supervision, Resources, Conceptualization. **Yawen Zheng:** Methodology, Investigation, Funding acquisition, Formal analysis. **Mingming Zhu:** Writing – review & editing, Supervision, Methodology, Funding acquisition, Conceptualization. **Dan Wang:** Methodology, Investigation, Formal analysis. **Junyao Wang:** Resources, Funding acquisition.

Declaration of competing interest

The authors declare that they have no known competing financial interests or personal relationships that could have appeared to influence

the work reported in this paper.

Acknowledgments

This work was supported by grants from Natural Science Foundation of Guangdong Province (No. 2024A1515012661), and Guangzhou Basic and Applied Basic Research Foundation (No. 2024A04J3828), Engineering and Physical Sciences Research Council, UK (EP/X03593X/1), and China Postdoctoral Science Foundation (No. 2024T170587, No. 2024M752134).

Appendix. The NH_3-based thermochemical recuperation power plant

Fig. A1 presents the schematic of the NH_3-based thermochemical recuperation power plant, which is proposed in previous study [39]. The NH_3-based thermochemical recuperation power plant includes power generation subsystem and thermochemical recuperation subsystem. NH_3 from storage tank is evaporated, and preheated by the exhaust gas. After preheating to the cracking temperature, the vaporous NH_3 is sent to the cracker, where NH_3 is decomposed into N_2 and H_2. Then the cracking production is mixed with compressed air and sent to the combustor. Following combustion, the high-temperature combustion production drives gas turbine for generation. The gas turbine inlet temperature is regulated by the air mass flow rate. The gas turbine exhaust gas is sent to supply heat for the endothermic NH_3 cracking reaction. Besides, the influence of gas turbine inlet temperature and pressure on the power generation efficiency was studied. Power efficiencies under different gas turbine inlet temperature and pressure are presented in Fig. A2. When the NH_3-based thermochemical recuperation power plant operates with gas turbine inlet temperature of 1000–1200 °C and pressure of 6–21 bar, the power generation efficiency ranges from 30.8 % to 42.8 %.

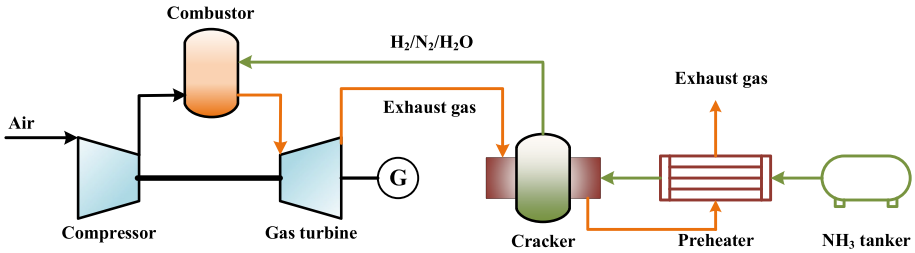


Fig. A1. The schematic of the NH_3-based thermochemical recuperation power plant.

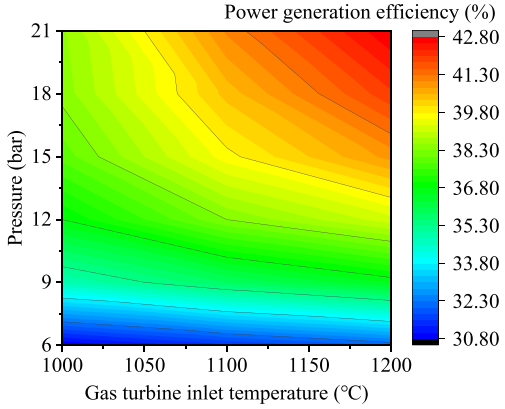


Fig. A2. Power efficiencies of the NH_3-based thermochemical recuperation power plant under different gas turbine inlet temperature and pressure.

Data availability

Data will be made available on request.

References

[1] Kim Y, et al. Novel cryogenic carbon dioxide capture and storage process using LNG cold energy in a natural gas combined cycle power plant. Chem Eng J 2023; 456:140980.
[2] Bao J, et al. Reduction of efficiency penalty for a natural gas combined cycle power plant with post-combustion CO_2 capture: integration of liquid natural gas cold energy. Energy Convers Manag 2019;198:111852.
[3] Sánchez A, et al. Evaluating ammonia as green fuel for power generation: a thermochemical perspective. Appl Energy 2021;293:116956.
[4] Khallaghi N, Hanak DP, Manovic V. Techno-economic evaluation of near-zero CO2 emission gas-fired power generation technologies: a review. J Nat Gas Sci Eng 2020;74:103095.
[5] Zheng Y, et al. Reduction potential of the energy penalty for CO2 capture in CCS. Front Energy 2023;17(3):390–9.
[6] Zheng Y, et al. Analysis and evaluation of the energy saving potential of the CO2 chemical absorption process. Int J Greenh Gas Control 2021;112:103486.
[7] Akeeb O, et al. Post-combustion CO2 capture via a variety of temperature ranges and material adsorption process: a review. J Environ Manag 2022;313:115026.
[8] Han R, et al. Progress in reducing calcination reaction temperature of Calcium-Looping CO2 capture technology: a critical review. Chem Eng J 2022;450:137952.
[9] Hanak DP, Anthony EJ, Manovic V. A review of developments in pilot-plant testing and modelling of calcium looping process for CO2 capture from power generation systems. Energy Environ Sci 2015;8(8):2199–249.
[10] Tan Y, et al. Conventional and optimized testing facilities of calcium looping process for CO2 capture: a systematic review. Fuel 2024;358:130337.
[11] Chen J, et al. Recent progress in calcium looping integrated with chemical looping combustion (CaL-CLC) using bifunctional CaO/CuO composites for CO2 capture: a state-of-the-art review. Fuel 2023;334:126630.
[12] Haaf M, et al. Operation of a 1 MWth calcium looping pilot plant firing waste-derived fuels in the calciner. Powder Technol 2020;372:267–74.
[13] Haaf M, et al. CO2 capture from waste-to-energy plants: techno-economic assessment of novel integration concepts of calcium looping technology. Resour Conserv Recycl 2020;162:104973.
[14] Strojny M, et al. Comparative analysis of CO2 capture technologies using amine absorption and calcium looping integrated with natural gas combined cycle power plant. Energy 2023;284:128599.

[15] Berstad D, et al. NGCC post-combustion CO2 capture with Ca/carbonate looping: efficiency dependency on sorbent properties, capture unit performance and process configuration. Int J Greenh Gas Control 2014;24:43–53.
[16] Berstad D, Anantharaman R, Jordal K. Post-combustion CO2 capture from a natural gas combined cycle by CaO/CaCO3 looping. Int J Greenh Gas Control 2012;11:25–33.
[17] Hu Y, Ahn H. Process integration of a Calcium-looping process with a natural gas combined cycle power plant for CO2 capture and its improvement by exhaust gas recirculation. Appl Energy 2017;187:480–8.
[18] Erans María HDP, Mir Jordi, Anthony Edward J, Manovic Vasilije. Process modelling and techno-economic analysis of natural gas combined cycle integrated with calcium looping. Therm Sci 2016;20(Issue suppl. 1):59–67.
[19] Cormos C-C. Techno-economic assessment of calcium and magnesium-based sorbents for post-combustion CO2 capture applied in fossil-fueled power plants. Fuel 2021;298:120794.
[20] Fu C, et al. Techno-economic analyses of the CaO/CaCO3 post-combustion CO2 capture from NGCC power plants, vol. 2; 2021.
[21] De Lena E, et al. Integrated calcium looping system with circulating fluidized bed reactors for low CO2 emission cement plants. Int J Greenh Gas Control 2022;114:103555.
[22] Greco-Coppi M, et al. Efficient CO2 capture from lime plants: techno-economic assessment of integrated concepts using indirectly heated carbonate looping technology. Carbon Capture Science & Technology 2024;11:100187.
[23] Martínez I, et al. Recent progress of the Ca-Cu technology for decarbonisation of power plants and carbon intensive industries. Int J Greenh Gas Control 2019;85:71–85.
[24] Martínez I, et al. Integration of a fluidised bed Ca–Cu chemical looping process in a steel mill. Energy 2018;163:570–84.
[25] Martini M, et al. Increasing the carbon capture efficiency of the Ca/Cu looping process for power production with advanced process schemes. Chem Eng J 2017;328:304–19.
[26] He S, et al. Proposal and thermodynamic investigation of pressurized calcium looping integrated with chemical looping combustion for tail-end CO2 capture in a retrofitted natural gas combined cycle power plant. Separ Purif Technol 2024;346:127464.
[27] Zhai R, et al. Thermodynamic analysis of CO2 capture by calcium looping process driven by coal and concentrated solar power. Energy Convers Manag 2016;117:251–63.
[28] Zhang X, Liu Y. Performance assessment of CO2 capture with calcination carbonation reaction process driven by coal and concentrated solar power. Appl Therm Eng 2014;70(1):13–24.
[29] Khosravi S, et al. Integration of a coal fired power plant with calcium looping CO2 capture and concentrated solar power generation: energy, exergy and economic analysis. Energy 2022;240:122466.
[30] Ferrario D, et al. Solar-driven calcium looping system for carbon capture in cement plants: process modelling and energy analysis. J Clean Prod 2023;394:136367.
[31] Moumin G, et al. CO2 emission reduction in the cement industry by using a solar calciner. Renew Energy 2020;145:1578–96.
[32] Kong H, et al. Life cycle assessment of ammonia co-firing power plants: a comprehensive review and analysis from a whole industrial chain perspective. Advances in Applied Energy 2024;14:100178.
[33] Tamura M, et al. Experimental investigation of ammonia combustion in a bench scale 1.2 MW-thermal pulverised coal firing furnace. Appl Energy 2020;277:115580.
[34] Kurata O, et al. Performances and emission characteristics of NH3–air and NH3CH4–air combustion gas-turbine power generations. Proc Combust Inst 2017;36(3):3351–9.
[35] Valera-Medina A, et al. Ammonia–methane combustion in tangential swirl burners for gas turbine power generation. Appl Energy 2017;185:1362–71.
[36] Su B, et al. Novel ammonia-driven chemically recuperated gas turbine cycle based on dual fuel mode. Appl Energy 2023;343:121184.
[37] Lesmana H, et al. NH3 as a transport fuel in internal combustion engines: a technical review. J Energy Resour Technol 2019;141(7).
[38] Wang C, et al. Tradeoff between the efficiency penalty and load depth in a coal-fired power plant with CO2 capture under partial load conditions. Energy Convers Manag 2023;278:116608.
[39] Pashchenko D, Mustafin R, Karpilov I. Ammonia-fired chemically recuperated gas turbine: thermodynamic analysis of cycle and recuperation system. Energy 2022;252:124081.
[40] Khan MN, et al. Integration of chemical looping combustion for cost-effective CO2 capture from state-of-the-art natural gas combined cycles. Energy Convers Manag X 2020;7:100044.
[41] Lee J-S, et al. Large-scale overseas transportation of hydrogen: comparative techno-economic and environmental investigation. Renew Sustain Energy Rev 2022;165:112556.
[42] Di Carlo A, Vecchione L, Del Prete Z. Ammonia decomposition over commercial Ru/Al2O3 catalyst: an experimental evaluation at different operative pressures and temperatures. Int J Hydrogen Energy 2014;39(2):808–14.
[43] Schakel W, et al. Impact of fuel selection on the environmental performance of post-combustion calcium looping applied to a cement plant. Appl Energy 2018;210:75–87.
[44] Pascual S, et al. Design and operational performance maps of calcium looping thermochemical energy storage for concentrating solar power plants. Energy 2021;220:119715.
[45] Alovisio A, et al. Optimizing the CSP-calcium looping integration for thermochemical energy storage. Energy Convers Manag 2017;136:85–98.
[46] Ortiz C, et al. Power cycles integration in concentrated solar power plants with energy storage based on calcium looping. Energy Convers Manag 2017;149:815–29.
[47] Yang D, Li S, He S. Zero/negative carbon emission coal and biomass staged co-gasification power generation system via biomass heating. Appl Energy 2024;357:122469.
[48] Dickmeis J, Kather A. The coal-fired oxyfuel-process with additional gas treatment of the ventgas for increased capture rates. Energy Proc 2014;63:332–41.
[49] Van der Spek M, et al. Techno-economic performance of state-of-the-art oxyfuel technology for low-CO2 coal-fired electricity production. Energy Proc 2017;114:6432–9.
[50] He S, Li S, Gao L. Proposal and energy saving analysis of novel methanol–electricity polygeneration system based on staged coal gasification method. Energy Convers Manag 2021;233:113931.
[51] Zheng Y, et al. Tracing the carbon capture energy distribution in a natural gas combined cycle power plant under variable operating conditions. Appl Therm Eng 2024;246:123000.
[52] Wang D, Sun Z, Xu Q, et al. Thermodynamic modeling and analysis of a Carnot battery system integrating calcium looping thermochemical energy storage with coal-fired power plant. Energy Convers Manag 2024;318:118888.
[53] Lim D, et al. Life cycle techno-economic and carbon footprint analysis of H2 production via NH_3 decomposition: a Case study for the Republic of Korea. Energy Convers Manag 2021;250:114881.
[54] Zhang X, Song P, Jiang L. Performance evaluation of an integrated redesigned coal fired power plant with CO2 capture by calcium looping process. Appl Therm Eng 2020;170:115027.
[55] Huang Z, et al. A novel biogas-driven CCHP system based on chemical reinjection. Energy 2024;297:131238.
[56] Chen Z, Wang Y, Zhang X. Energy and exergy analyses of S–CO_2 coal-fired power plant with reheating processes. Energy 2020;211:118651.
[57] Xue X, et al. Proposal and evaluation of a hydrogen and electricity cogeneration system based on thermochemical complementary utilization of coal and solar energy. Energy Convers Manag 2023;291:117266.
[58] Li J, et al. Efficient coal-based power generation via optimized supercritical water gasification with chemical recuperation. Appl Therm Eng 2024;238:122164.
[59] Lee K, Liu X, Vyawahare P, et al. Techno-economic performances and life cycle greenhouse gas emissions of various ammonia production pathways including conventional, carbon-capturing, nuclear-powered, and renewable production. Green Chem 2022;24(12):4830–44.
[60] Wang L, Zhang Y, Pérez-Fortes M, et al. Reversible solid-oxide cell stack based power-to-x-to-power systems: comparison of thermodynamic performance. Appl Energy 2020;275:115330.



https://dspace.org/

Thermodynamic analysis of decarbonizing NGCC power plants by the tail-end green ammonia-driven calcium looping

He, Song; Zeng, Xuelan; Zheng, Yawen; Zhu, Mingming; Wang, Dan ...

2025-01-01
Elsevier
https://doi.org/10.1016/j.energy.2024.134147
He S, Zeng X, Zheng Y, et al., (2025) Thermodynamic analysis of decarbonizing NGCC power plants by the tail-end green ammonia-driven calcium looping. Energy, Volume 314, January 2025, Article number 134147

Downloaded from a DSpace repository. https://dspace.org/